Available online at www.sciencedirect.com

ScienceDirect

Energy Procedia 1 (2009) 1381–1386

Energy Procedia

www.elsevier.com/locate/procedia

GHGT-9

Foaming in amine-based CO_2 capture process: experiment, modeling and simulation

Bhurisa Thitakamol, Amornvadee Veawab*, Adisorn Aroonwilas

Faculty of Engineering, University of Regina, Saskatchewan S4S 0A2, Canada

Abstract

This work provides a parametric study on foaming behavior in the carbon dioxide (CO_2) absorption process using aqueous monoethanolamine (MEA) solutions. Foaming tendency was experimentally evaluated using the pneumatic method modified from ASTM standard, and reported in terms of foaminess coefficient ($\sum$). Results show that $\sum$ increases and eventually decreases with MEA concentration and CO_2 loading. A higher solution temperature reduces $\sum$. Most tested degradation products and corrosion inhibitors enhance foam tendency. A foaming model was developed to predict pneumatic steady-state foam heights. It consists of an empirical correlation for foam height prediction and a series of subroutine modules for physical property estimation. The model fits well with the experimental foam data with R^2 of 0.88.

Keywords: CO_2 absorption; CO_2 capture; alkanolamine; amine; foaming

1. Introduction

Foaming is a severe operational problem in acid gas absorption process using aqueous alkanolamine solutions. It occurs during plant start-up and operation in both absorber and regenerator [1-9] and is caused by high gas velocities, sludge deposits on gas contactors, and process contaminants entering the process with feed gas and makeup water, or generated within the process through reactions of alkanolamine degradation. Based on plant experiences, foaming impacts integrity of plant operation, causing excessive loss of absorption solvents, premature flooding, reduction in plant throughput, off-specification of products, and high absorption solvent carryover to downstream plants. To date, the knowledge of foaming in this process is limited for oil and gas operations and even more limited for the application of CO_2 capture from industrial flue gas for the purpose of greenhouse gas emission reduction. This work therefore aims at two objectives: 1) obtaining comprehensive foaming information from

* Corresponding author. Tel.: +1-306-585-5665; fax: +1-306-585-4855.
E-mail address: veawab@uregina.ca.

doi:10.1016/j.egypro.2009.01.181

bench-scale experiments under well-simulated environments to reveal effects of process parameters on foaming and 2) developing a foaming model for prediction of foam height. The results from this work would benefit practitioners in developing cost-effective means of foaming prevention and control.

2. Experiments

Foaming experiments were carried out using the pneumatic method modified from the standard ASTM D892 [10]. Figure 1 illustrates a schematic diagram of experiment setup. Details of experimental setup and procedure can be found in Thitakamol and Veawab (2008) [11]. Prior to each experiment, the test solution was placed at a given volume into a test cell and then heated in a temperature bath to a set temperature. A metal diffuser was inserted into the heated test cell and left for approximately 5 minutes to be saturated with the test solution. Nitrogen (N_2) was then introduced to a drying column to remove moistures before entering a mass flow meter. The test solution was vigorously bubbled by N_2 through the gas diffuser with a blowing time of 25 min ± 5 seconds. The blowing time was first counted when the first N_2 bubble raised from the gas diffuser. The N_2 gas was eventually released to the atmosphere from the outlet of the test cell. The concentration of alkanolamine solution as well as its CO_2 loading, conductivity and pH were determined before and after each experiment to ensure no changes in the solution constituents due to the alkanolamine degradation products or the variation in operating condition. During the blowing time, the foam volume above the gas dispersion layer was recorded every minute. The average foam volumes were used instead of the actual foam volume to reduce errors due to data readings. A foaminess coefficient (Σ) was calculated by using the following equation [12].

$$\Sigma = \frac{\upsilon_o}{G} \tag{1}$$

where υ_o is average steady foam volume (m^3) and G is gas (N_2) flow rate (m^3/hr).

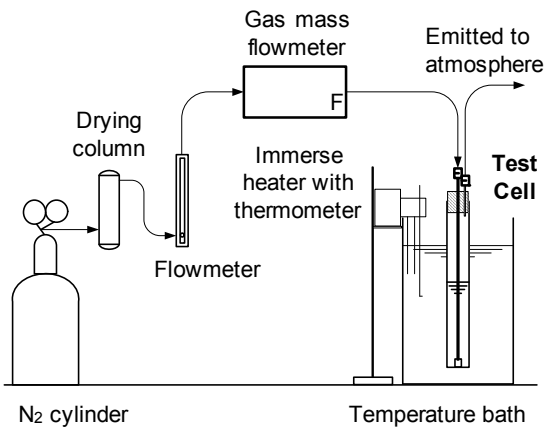

Figure 1 Schematic diagram of foaming experimental setup

3. Experimental results and discussion

A parametric study was performed under a wide spectrum of operating conditions as summarized Table 1. The tested parameters were solution volume, gas flow rate, alkanolamine concentration, CO_2 loading of solution, solution temperature, degradation product of alkanolamine, and corrosion inhibitor. All experimental runs were

replicated and found reproducible with a standard deviation of the foaminess coefficient of 0.15 min. The results are shown in Figure 2. Detailed explanation of the results can be found in Thitakamol and Veawab [11].

Table 1 Summary of tested parameters and operating conditions

Parameter	Range
N_2 flow rate	1.2×10^{-3} – 9.3×10^{-3} m^3/hr
Solution volume	2.0×10^{-4} – 7.0×10^{-4} m^3
Alkanolamine concentration	2.0 – 7.0 kmol/m^3
CO_2 loading	0.10 – 0.55 mol/mol
Solution temperature	40 – 90ºC
Degradation product of MEA	acetic acid, ammonium thiosulfate, bicine, formic acid, glycolic acid, hydrochloric acid, malonic acid, oxalic acid, sodium chloride, sodium sulfite, sodium thiocyanate, sodium thiosulfate, sulfuric acid
Corrosion inhibitor	copper carbonate, sodium metavanadate, sodium sulfite

Effect of gas flow rate: An increase in gas flow rate initially decreases Σ. This is because the increasing turbulence created by the increasing gas flow rate disrupts foam formation and reduces foam stability. As N_2 flow rate is further increased to 4.80×10^{-3} m^3/hr (80 cm^3/min) or greater, Σ reaches stabilization. This suggests that the volume of foams proportionally increases with N_2 flow rate.

Effect of solution volume: Foam formation does not occur when solution volume is 2.0×10^{-4} m^3. This is due to the inadequate hydrostatic force to resist the buoyancy force of a N_2 bubble. Once the solution volume increases to more than 2.0×10^{-4} m^3, foams are produced and Σ increases with solution volume. This is because the increase in solution volume leads to an increase in hydrostatic force which in turn reduces the turbulence caused by the bubble detachment from the diffuser. As the solution volume is further increased from 4.0×10^{-4} to 7.0×10^{-4} m^3, Σ becomes invariant. This is because the increasing hydrostatic force overcomes the turbulence caused by the bubble detachment, or makes such turbulence insignificant.

Effect of MEA concentration: Σ initially increases with MEA concentration and then declines. The increase in Σ with MEA concentration is due to the decrease in surface tension of solution and the increase in density and viscosity of MEA solution.. The decrease in Σ is a result of creaming process where bulk viscosity plays a significant role on the rising bubbles through the liquid phase to form a foam layer. The decrease in Σ is also caused by a reduction of foam stability due to an increase in surface viscosity of the solution.

Effect of CO_2 loading: An increase in CO_2 loading generally increases Σ. This is due to surface tension and density of the solution. As CO_2 loading increases, surface tension decreases and solution density increases. This results in a reduced surface force and an increased buoyancy force, thus promoting foam formation and causing a greater Σ. In addition to the increasing trend of Σ, Σ tends to decrease after the CO_2 loading is increased to a certain value. This is primarily due to the influence of solution viscosity, which becomes more significant than those of surface tension and density.

Effect of solution temperature: As solution temperature is increased, Σ decreases considerably. This is a result of poor foam stability, which is caused by a reduced bulk viscosity and a turbulence flow created by the vigorous movement of molecules at an elevated temperature.

Effect of MEA degradation products: The solutions containing degradation products (except sulfuric acid) provide greater Σ values than those without degradation products. Ammonium thiosulfate induces the highest foam volume and Σ, followed by glycolic acid, sodium sulfite, malonic acid, oxalic acid, sodium thiocyanate, sodium

chloride, sodium thiosulfate, bicine, hydrochloric acid, formic acid, acetic acid and sulfuric acid. The increase in Σ is due to the formation of anionic surfactants in the presence of sulfate (OSO_3^-), sulfonate (SO_3^-) and carboxylate (COO^-) functioning as a hydrophilic group. The anionic surfactants reduce surface tension of the solution, thus encouraging foam formation. The results also show that the presence of chloride ion increases Σ. This is probably because the chloride ion reduces surface tension by neutralizing the ionic products resulted from the reaction between CO_2 and MEA, which in turn enhances foam formation.

Effect of corrosion inhibitor: Sodium metavanadate and copper carbonate increase Σ and of which sodium metavanadate induces a greater effect, whereas sodium sulfite has no apparent effect. This is because the surface tension values of MEA solution are reduced when sodium metavanadate and copper carbonate are added.

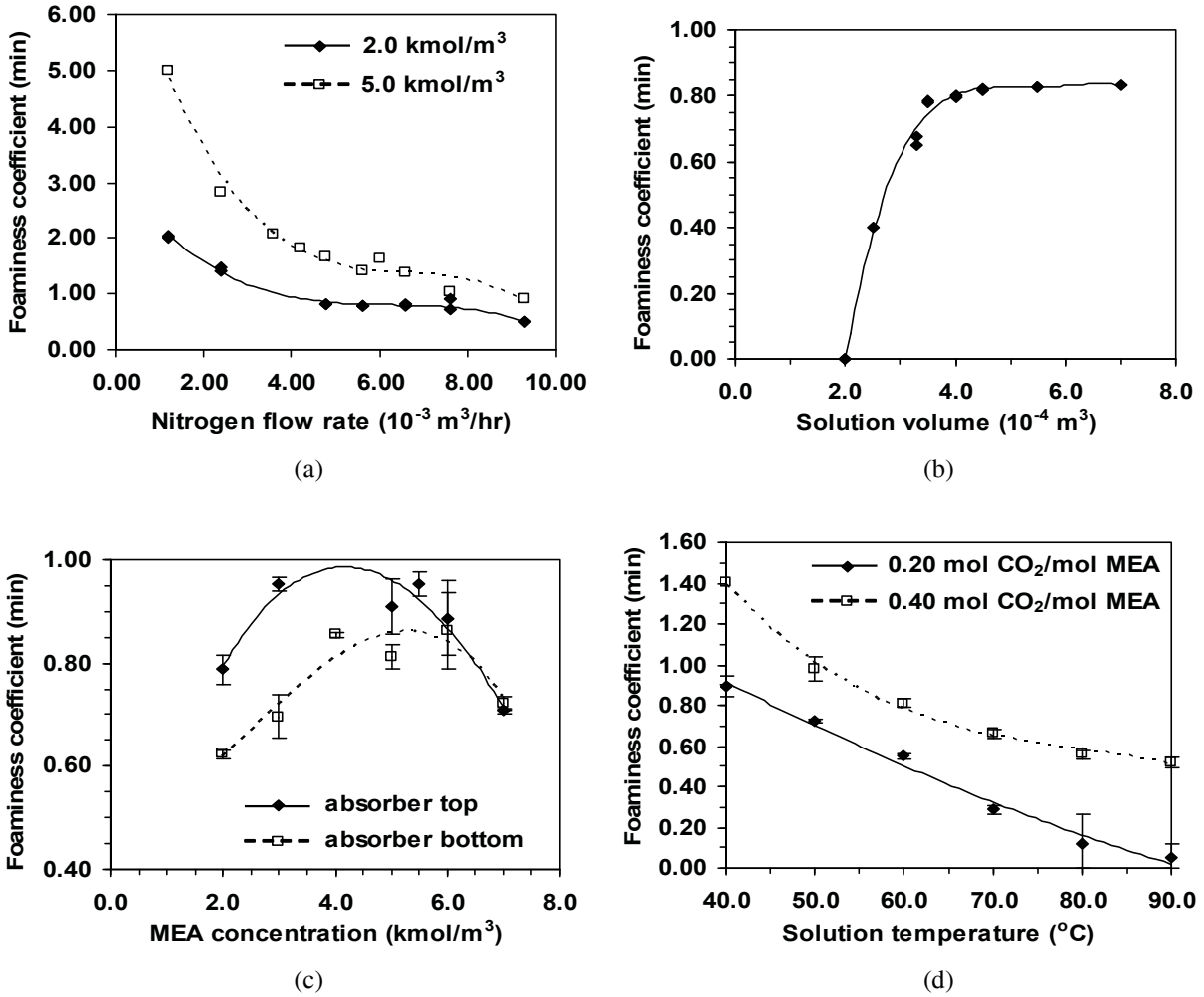

Figure 2 Effect of process parameters on foaminess coefficient **(a)** Gas flow rate (MEA concentration = 2.0 and 5.0 kmol/m^3, solution volume = 4.0×10^{-4} m^3, CO_2 loading = 0.40 mol/mol and solution temperature = 40°C), **(b)** Solution volume (MEA concentration = 2.0 kmol/m^3, N_2 flow rate = 5.64×10^{-3} m^3/hr, CO_2 loading = 0.40 mol/mol and solution temperature = 40°C), **(c)** MEA concentration (N_2 flow rate = 5.64×10^{-3} m^3/hr, solution volume = 4.0×10^{-4} m^3, *absorber top condition*: CO_2 loading = 0.20 mol/mol; solution temperature = 40°C, *absorber bottom condition*: CO_2 loading = 0.40 mol/mol; solution temperature = 60°C), and **(d)** Solution temperature (MEA concentration = 5.0 kmol/m^3, N_2 flow rate = 5.64×10^{-3} m^3/hr, solution volume = 4.0×10^{-4} m^3 and CO_2 loading = 0.20 & 0.40 mol/mol)

4. Foaming model

A foaming model was developed to predict pneumatic steady-state foam heights. The model was built on Pilon *et al.* (2001) [13] model and our experimental foam data. The foaming model consists of an empirical correlation (Equation 2) and a series of subroutine modules for estimations of bubble radius and physical properties (density of gas and liquid, solution viscosity and surface tension). The foam height correlation comprises parameters (including bubble radius, surface tension of liquid, viscosity of liquid, difference in density of gas and liquid and superficial gas velocity), constants K of 4394 and n of -1.30, and dimensionless Ca, Re and Fr in ranges of 2.0×10^{-3} – 6.3×10^{-2}, 5.0 – 276.4 and 0.01 – 0.89, respectively. The model fits well with the experimental data as indicated by R^2 of 0.88 and an error of up to 14%.

$$H_o = 4394\frac{\gamma}{r_o^{1.60}}\left(\frac{(\mu_L j)^{0.30}}{(\Delta\rho g)^{1.30}}\right) \quad (2)$$

Sensitivity analysis was carried out to rank the parametric effects on the foam height. For each parameter, a curve was plotted between % change in parameter and foam height index. The value of the parameter of interest was increased by 10% increment from its minimum to maximum while the rest of the process parameters were fixed constant. The foam height index is defined as a ratio of the predicted foam height at a new value of parameter to the predicted foam height at the minimum value of parameter. As shown in Figure 3, among process parameters, solution volume is the most influential on the foam height, followed by solution temperature. Among physical properties, the foam height is the most sensitive to liquid viscosity followed by liquid density and surface tension while it is not sensitive to gas density.

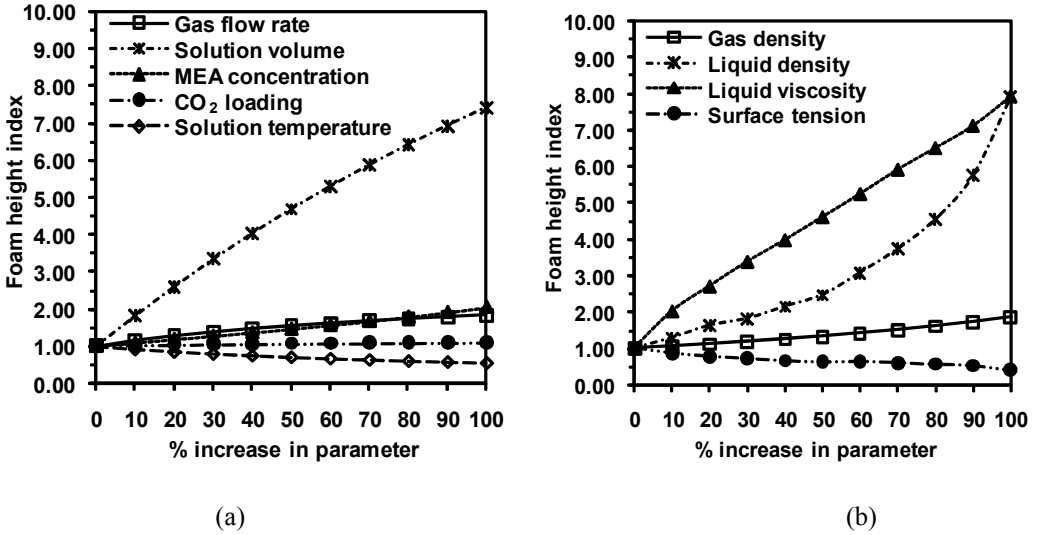

Figure 3 Sensitivity analysis of **(a)** process parameters and **(b)** physical properties on foam height index

5. Conclusions

Foaming behavior in the MEA-based CO_2 absorption process is influenced by process parameters. Foam height increases with gas flow rate, solution volume, CO_2 loading, MEA concentration, but decreases with solution temperature. Most degradation products and corrosion inhibitors in aqueous MEA solutions enhance foaminess coefficient, except for sulfuric acid. Physical properties, namely surface tension, density and viscosity of solution, play a significant role in foaming tendency through foam formation and foam stability. A foaming model for this process was successfully developed. It comprises an empirical correlation for predicting pneumatic steady-state

foam heights and a series of subroutine modules for physical property estimation. The model fits well with the experimental foam data with R^2 of 0.88. Compared to other process parameters, solution volume is the most influential on the foam height, followed by solution temperature. Among physical properties, the foam height is the most sensitive to liquid viscosity followed by liquid density and surface tension, but not sensitive to gas density.

Acknowledgments

The Natural Sciences and Engineering Research Council of Canada (NSERC) is gratefully acknowledged for generous financial support.

References

1. D. Ballard, Hydrocarbon Process. 45 (1966) 137 – 144.
2. D. Ballard, Proceedings of Laurance Reid Gas Conditioning Conference. (1986) A1 – A38.
3. R. F. Smith, Oil Gas J. July 30 (1979A) 186 – 192.
4. N. P. Lieberman, Oil Gas J. May 12 (1980), 115 – 120.
5. M. M. Keaton and M. J. Bourke, Hydrocarbon Process. 62 (1983) 71 – 73.
6. J. Thomason, Hydrocarbon Process. 64 (1985) 75 – 78.
7. C. R. Pauley, Chem. Eng. Prog. 87 (1991) 33 – 38.
8. E. J. Stewart and R. A. Lanning, Hydrocarbon Process. 73 (1994) 67 – 81.
9. M. A. Abdi, M. M. Golkar and A. Meisen, Hydrocarbon Process. 80 (2001) 102C – 102I.
10. American Society for Testing and Materials (ASTM), ASTM D892-Standard Test Method for Foaming Characteristics of Lubricating Oil, ASTM, 1999.
11. B. Thitakamol and A. Veawab, Ind. Eng. Chem. Res. 47 (2008) 216 – 225.
12. J. J. Bikerman, Foams, Springer-Verlag, New York, 1973.
13. L. Pilon, A. G. Fedorov and R. Viskanta, J. Colloid Interface Sci. 242 (2001) 425 – 436.